

UNCLASSIFIED

AD 407 931

DEFENSE DOCUMENTATION CENTER

FOR

SCIENTIFIC AND TECHNICAL INFORMATION

CAMERON STATION, ALEXANDRIA, VIRGINIA



UNCLASSIFIED

NOTICE: When government or other drawings, specifications or other data are used for any purpose other than in connection with a definitely related government procurement operation, the U. S. Government thereby incurs no responsibility, nor any obligation whatsoever; and the fact that the Government may have formulated, furnished, or in any way supplied the said drawings, specifications, or other data is not to be regarded by implication or otherwise as in any manner licensing the holder or any other person or corporation, or conveying any rights or permission to manufacture, use or sell any patented invention that may in any way be related thereto.

④ \$5,600
⑤ 716300

⑥ AN EXPERIMENTAL INVESTIGATION OF
HEAT TRANSFER AND PRESSURE EFFECTS
ON LONGITUDINAL COMBUSTION INSTABILITY
IN A ROCKET MOTOR USING PREMIXED
GASEOUS PROPELLANTS,

- ⑦ NA
- ⑧ NA
- ⑨ NA
- ⑩ Jun 63,
- ⑪ 50 P.
- ⑫ NA
- ⑬-⑭ NA

⑩ by

Submitted by: Walter J. Schob Jr.
Walter J. Schob Jr.,
Captain, USAF

Approved by: Irvin Glassman
Irvin Glassman
Associate Professor

A thesis submitted to the Department of Aeronautical
Engineering of Princeton University in partial
fulfillment of the requirements for the degree of
Master of Science in Engineering.

② 4. June 1963
② Master's thesis

PRINCETON UNIVERSITY
Princeton, New Jersey

ACKNOWLEDGMENTS

The author wishes to extend his thanks to Mr. Maurice Webb, who helped make this report possible through his extensive technical advice, assistance and encouragement throughout the research, and to Professors Luigi Crocco and Irvin Glassman who have overall cognizance over the program and extended help when needed.

His gratitude is also extended to Mr. Joseph Sivo and Mr. Steven Marquardt, whose technical efforts contributed to the timely performance of the experiments in the report.

The author is very proud to have been selected by the United States Air Force Institute of Technology for the opportunity to further his education at the Guggenheim Laboratories for Aerospace Propulsion Sciences at Princeton University, and acknowledges the Financial Support of the United States Air Force, Office of Scientific Research Grant AF-AFOSR 111-63, which made this investigation possible.

ABSTRACT

Several experiments were performed to further investigate the high frequency, longitudinal, combustion instability regions and their limits encountered during operation of a rocket motor using gaseous propellants. These experiments were designed to change the heat transfer rate to the injector face by changing heat transfer properties of the propellant gases and injector configuration; to measure the axial temperature profile in the combustion region; to study the effects of changing the mean chamber pressure; and to measure the wave form of the oscillatory pressure in the combustion chamber.

It was concluded that no change in the stability regions occurred as a result of changing the injector configuration or the mean chamber pressure; a change in the equivalence ratios of the unstable regions occurred when the heat transfer properties of the propellant gases were changed but that no change in the actual combustion chamber temperature was associated with the equivalence ratio change; combustion was completed in a distance less than 1.5 inches from the injector face and that the oscillatory pressure in the combustion chamber had the form of a shock wave.

TABLE OF CONTENTS

| | | |
|---------|---|-----|
| | TITLE PAGE | i |
| | ACKNOWLEDGMENT | ii |
| | ABSTRACT | iii |
| | TABLE OF CONTENTS | iv |
| | LIST OF FIGURES | vi |
| CHAPTER | 1. INTRODUCTION | 1 |
| | A. Gas Rocket Motor | 2 |
| | B. Background | 2 |
| | C. Unstable Regions and Limits | 5 |
| | D. Definitions | 5 |
| | 11. APPARATUS DESCRIPTION | 6 |
| | A. Basic Rocket Installation | 6 |
| | B. Propellant Metering System | 6 |
| | C. Mixing Chamber | 7 |
| | D. Combustion Chamber Injectors | 7 |
| | E. Combustion Chamber | 8 |
| | F. Nozzle | 9 |
| | G. Temperature and Pressure Measurements in Combustion Chamber | 9 |
| | H. Flashback | 10 |
| | I. Starting Problem | 12 |
| | 111. DESCRIPTION OF EXPERIMENTS | 13 |
| | A. Introduction | 13 |
| | B. Increasing Heat Transfer Rate to Injector | 14 |

| | |
|--|----|
| C. Decreasing Heat Transfer Rate to Injector | 21 |
| D. Increasing Heat Transfer Properties of Combustion Gases | 24 |
| E. Combustion Gas Temperature at Unstable Region Limits | 33 |
| F. Effect of Chamber Pressure Variation | 39 |
| G. Wave Form of Unstable Oscillations | 41 |
| IV. CONCLUSIONS | 46 |
| REFERENCES | 49 |
| FIGURES | 51 |

LIST OF FIGURES

Figure No.

1. Schematic of Oscillating Heat Transfer Mechanism
2. Impingement Injector Plate
3. Mixing Chamber Section
4. Injectors
5. First Section of Combustion Chamber With Nozzle Inserted
- 6.] Instrumentation and Flow Schematic
7. Stability Map, Hydrogen Fuel and Air Oxidizer
8. Stability Map, Hydrogen Fuel and Helium-Oxygen Oxidizer
9. Heat Transport Properties of Combustion Gases
10. Thermocouple Installation in Combustion Chamber
11. Measured Axial Temperature Profiles Through Combustion Zone
12. Wave Form of Unstable Oscillation

CHAPTER 1

INTRODUCTION

The problem of combustion instability has plagued the rocket motor industry since its birth, with increasing concern since the advent of the space age (1).

When periodic pressure oscillations begin in the combustion chamber of a rocket engine designed for maximum performance, high thrust and minimum weight, the increased rates of localized heat transfer and increases values of oscillating chamber pressures almost invariably exceed design limitations and motor destruction follows.

The ultimate goal of the many investigations being carried on in the field of combustion instability would be the complete elimination of combustion instability. A welcome second choice would be the ability to predict the onset of combustion instability using common rocket motor parameters, such as: propellant mixture ratio, injector configuration and combustion chamber dimensions, pressures and temperatures, so that these regions might be designed out of the operational envelope of the rocket motor.

Another goal of both theoretical and experimental investigation would be to find a suitable method to scale the results of tests with small rocket motors to large rocket motors. Testing large motors is an expensive

operation especially if the test ends in destruction of the motor.

A. Gas Rocket Motor

The gas rocket motor was designed and built at Princeton in 1959 to study the problems of combustion instability in a simpler system than a liquid motor would allow. Some of the physical processes peculiar to the liquid rocket motor, such as atomization, vaporization and mixing, are removed by the use of premixed gaseous oxidizer and fuel. Therefore, any instabilities encountered would have to be attributed to phenomena occurring in or related to the gas phase of the propellants.

B. Background

Previous investigation with the gas rocket at Princeton University did not quantitatively establish the validity of the theoretical model chosen by Crocco and Bortzmeyer (2) to describe the driving mechanism of the instability.

The proposed driving mechanism was one in which an oscillating heat transfer to the injector coupled with an oscillation in the combustion chamber to produce combustion instability. This idea for the mechanism is similar to the burning of solid propellants where heat and mass transfer processes are the controlling processes in combustion instability.

A description of this mechanism follows with the aid of

Figure 1, which is reproduced directly from Reference 2. T_0 is the temperature of the face of the injector on the combustion chamber side, and since the gaseous propellants are considered to be in thermal equilibrium with the injector, T_0 is also the temperature of the gases when they enter the combustion chamber.

T_1 is the temperature of the gases after they have been burned and are still but a small distance away from the injector. The mechanism states that if, at a given time, the pressure near the injector plate increases due to some disturbance, the heat transfer to the injector will also increase. This increase in heat transfer will cause the injector temperature (and injected gas temperature) T_0 to rise after a proper time lag caused by the inertia of the transfer process.

Then, due to the increase in T_0 , and again after the proper time lag, the final temperature of the combustion gases, T_1 , will also rise. Note that as T_0 rises, the heat transfer to the injector must decrease because of the decrease in $T_1 - T_0$, the driving force of the heat transfer. Thus, it can be seen that if the time lags of the heat and mass flow transfer processes are properly related to the period of oscillation of the combustion chamber, the energy released from the combustion process can oscillate in phase with the natural mode of the combustion chamber. That is, the combustion

will be unstable.

In early experiments by Pelmas (3), qualitative agreement was obtained between the theoretical predictions using this model and experimental results. At the time, it was felt that more experimental data, relating the effects of heat transfer, had to be obtained before any quantitative comparison could be made.

Later experiments by Bertrand (4), confirmed a modification of the theory which predicted all frequencies and harmonics which had been experimentally observed.

All of these experiments raised questions about the relationship between the unstable regions encountered and parameters such as: heat transfer to the injector, heat transport properties of the combustion gases, and combustion chamber pressures and temperatures.

The experiments in this report were conducted to further test the Crocco-Bortzmeyer theory and attempt to gain a deeper understanding, through experimental observations, of causes and effects of the instabilities in the gas rocket. This might give a better idea of how to modify the existing theory, or possibly provide a basis for a new theory utilizing a different combustion model.

This report will cover observed changes in the unstable regions and their limits caused by changing injector configuration, chamber conditions, motor length and propellants.

C. Unstable Regions and Limits

The regions of high frequency, longitudinal instability and their limits referred to throughout this report are described by a "stability map" on a graph of equivalence ratio versus motor length. Holding the motor length and combustion chamber pressure constant, combustion instabilities occur while traversing through certain ranges of equivalence ratios.

When these unstable ranges of equivalence ratios are joined together with motor length as the abscissa of the graph, an unstable region is formed with definite values of equivalence ratio as limits. (See Figures 7 and 8.)

D. Definitions

At the onset, it would be of value to restate the definitions of the terms "equivalence ratio", "combustion instability" and "unstable region limit" as used throughout this report.

The equivalence ratio, ϕ , is the actual mass flow rate ratio of oxidizer to fuel to the theoretical stoichiometric (st.) mass flow rate ratio of oxidizer to fuel.

$$\frac{\dot{m}_o}{\dot{m}_f} / \left(\frac{\dot{m}_o}{\dot{m}_f} \right)_{st.} = \phi$$

Combustion instabilities are harmonic, longitudinal chamber pressure oscillations with well defined frequencies of finite amplitude, and the limit of an unstable region is the border at which there is a transition between stable and unstable combustion.

CHAPTER 11

APPARATUS DESCRIPTION

A. Basic Rocket Installation

The gas rocket installation is composed of the following basic components: a propellant metering system, a propellant mixing chamber, an injector, a combustion chamber and a nozzle. Provisions are available for measuring and recording combustion chamber pressures, temperatures and propellant flow rates during test runs.

The motor is uncooled with thick copper walls, which serve the dual purpose of cooling by virtue of a large thermal capacity, and providing structural integrity under conditions of high localized heat transfer rates and oscillating pressures.

The motor was designed so that the combustion chamber length, pressure transducer location and injectors could be readily changed. Different propellant combinations at varying mixture ratios could be accurately controlled by the propellant feed system.

B. Propellant Metering System

Critical flow orifices were used to meter propellants to the gas rocket. The orifices were flow calibrated when the equipment was originally built. To facilitate rapid changing of propellant mass flows between test runs, the orifices were mounted in manifolds with a separate valve to open and close

each orifice (Figure 6).

Stagnation pressure of the propellants was measured upstream of the critical flow orifices by bourdon gauges with a standard accuracy of 0.5% between 400 and 2000 psig and calibrated to an accuracy of ± 1 psi. Pressures were also measured downstream of the orifices to verify the differential needed across the orifice to assure choked flow.

Stagnation temperatures of the propellants were measured upstream of the orifices by copper-constantan thermocouples.

C. Mixing Chamber

Each propellant gas entered the mixing chamber through an impingement type injector consisting of four sets of like-on-unlike orifices inclined at 30 degrees to each other which provided initial rough mixing (Figure 2). Complete mixing, before injection into the combustion chamber, was accomplished by passing the roughly mixed gas through a bed of tightly packed 0.25 inch stainless steel balls. A screen prevented the balls from touching the rear face of the chamber injector (Figure 3).

D. Combustion Chamber Injectors

The thoroughly mixed propellants passed through a 0.25 inch thick, 1.75 inch diameter copper injector which was force fitted into the downstream end of the mixing chamber and held firmly in place by bolting the first section of the combustion

chamber against the injector.

Two types of injectors were used in the following experiments, a six orifice double triplet injector and a ten orifice injector (Figure 4).

E. Combustion Chamber

The combustion chamber was constructed of five inch copper sections with a wall thickness of 0.75 inches. A stainless steel liner with an inner diameter of 1.5 inches was press fitted into the core of each section. Using these sections, and a variable length (0 to 5 inch) nozzle section, combustion chamber lengths between 1.625 and 40 inches could be constructed.

Combustion chamber sections were joined together using Marmon clamps with Garlock spiral wound gaskets to seal the flange faces against pressure leaks. These flange faces were often broken and resealed to change motor length and to inspect visually conditions inside the chamber. Pressure leaks that originated from small deformations in the Garlock gaskets were stopped by placing a 0.002 inch aluminum foil gasket between sections before reclamping the sections.

Since propellant mass flow was a very important parameter during all experiments, the presence of pressure leaks, either of the propellant or of the combustion products could not be tolerated.

Propellant leaks cause erroneous calculation of the

equivalence ratios at which instabilities are recorded and combustion product leaks cause errors in the total mass flow needed to maintain a constant chamber pressure.

Before each set of runs and in the middle of a long sequence of runs, the motor was pressure tested to assure that no leaks had developed in the system.

F. Nozzle

The water cooled, convergent-divergent nozzle had a 0.22 inch throat diameter and the convergent portion of the nozzle had a half angle of 30 degrees. The cooling water entered the nozzle at the exit section and was forced forward through the nozzle walls and out the entrance section under 100 psi of pressure.

The nozzle could be secured at any length in the five inch nozzle section, which was of similar construction to a combustion chamber section. An "O" ring seal prevented pressure leaks past the sliding portion of the nozzle. A special adaptor (Figure 5) made it possible to slide the nozzle into the first five inch section of the combustion chamber.

G. Temperature and Pressure Measurements in Combustion Chamber

The thermocouples used to measure the combustion temperatures in the first five inch section of the combustion chamber (Chapter III-E) were connected to a six position thermocouple switch the output of which was connected to a

chart recorder. In this manner each thermocouple could be interrogated individually or in a prescribed sequence.

Steady combustion chamber pressures were measured with a Flader P6HD transducer which sensed the pressure through an 18 inch tube connected to the first five inch section of the combustion chamber. All steady state data taken during a test run was recorded in a centrally located recording room on Leeds and Northrup Speedomax recorders.

Transient chamber pressures and corresponding frequencies and amplitudes, measured by a Dynisco PT49 transducer, were displayed on an oscilloscope for immediate determination of unstable combustion during the run and recorded on a seven channel Ampex tape recorder for later analysis.

Since extra channels were available on the tape recorder, a time history of the upstream propellant pressure settings was verbally recorded as each pressure setting was obtained.

All time histories were synchronized with the start of the test portion of the run by a timing marker, which was triggered manually when desired, on all speedomax and tape recorders.

Transducer and recording equipment peculiar only to the experiment performed in Chapter III-G will be described at the beginning of that chapter.

H. Flashback

To prevent combustion flashback into the mixing chamber

from remaining undetected by the oxidizer shut-off safety circuit, 0.50 inch diameter plexiglass windows (Figure 3), were installed in the mixing chamber replacing 0.38 inch diameter windows.

The greater window area increased the sensitivity of the safety circuit to the flashback generated light of combustion in the mixing chamber and eliminated undetected flashback by actuating the safety circuit sooner after flashback occurred, preventing damage to the mixing chamber.

It was found using the propellant combinations described in the following experiments, that when a succession of flashbacks occurred, the cause could invariably be traced to a loose fitting injector.

Even though the first combustion chamber section was butted against the face of the injector, combustion gases could flow between the steel inner liner and the copper walls back upstream to the loose injector, then around the edge of the injector into the mixing chamber.

This flow pattern was evidenced by discoloration on the outside of the steel inner lining, from the holes cut for the transducer and spark plug ignitors, to the upstream end of the first combustion chamber section. The edges of the loose injectors were also discolored after a series of flashbacks.

By replacing the injector, or silver soldering the injector in the end of the mixing chamber, flashback was

prevented. It was also found that an aluminum foil gasket between the first section of the combustion chamber and the injector also prevented flashback caused by a slightly loose fitting injector.

I. Starting Problems

When the six orifice double triplet injector (Figure 4a) was used, the motor could not be started with the orifices aligned 90 degrees to the spark plug ignitors. By rotating the plug 90 degrees, the motor could be started easily and this problem was assumed to be caused by a peculiar recirculation pattern of propellants which either presented the ignitor with a non-combustable mixture or very little mixture at all. No further investigation of this effect was carried out.

CHAPTER 111

DESCRIPTION OF EXPERIMENTS

A. Introduction

This report covers six separate experiments performed to further investigate the combustion instability regions and their limits encountered during operation of the gas rocket. Individual experimental results are discussed at the end of each experiment and conclusions drawn from all six experiments are discussed in Chapter 1V.

The theory of Crocco and Bortzmeyer (2), associated the occurrence of combustion instability with the amount of heat transfer to the injector as discussed in Chapter 1. The first three experiments studied the effects of changing the heat transfer rate to the injector.

In the first experiments, heat transfer to the injector was increased, in the second, the heat transfer to the injector was decreased and in the third, the heat transfer properties of the combustion gases were increased.

Results of these experiments led to the next two experiments in this report, namely, an investigation of the actual combustion chamber temperature at the unstable region limits, and the effects of combustion chamber pressure on these limits.

A shock wave theory of combustion instability was proposed at Princeton University in March, 1963, (17) and the

last experiment was performed to measure and photographically record the pressure wave form during combustion instability, upon which the theory was predicated.

B. Increasing Heat Transfer Rate to Injector

This experiment was performed to see what effect a large increase in the heat transfer rate to the injector would have on the unstable regions and limits previously found by Pelmas (3) using porous injectors and Bertrand (4) using ceramic coated and water cooled injectors containing various numbers of orifices.

In the theory of Crocco and Bortzmeyer (2), combustion instabilities are predicted as a function of a dimensionless heat transfer coefficient, \bar{h} . This coefficient depends only on three parameters of the combustion gases, the heat transfer coefficient, the specific heat and the total mass flow ($\bar{h} = \frac{h}{\dot{m} C_p}$).

To keep the heat transfer coefficient independent of any recirculation from the combustion zone to the injector, a mathematical model for an injector which delivered one dimensional, uniform velocity, pre-mixed propellant flow to the combustion chamber was chosen for the theory.

For this reason, injectors in past experiments were designed to simulate the model as closely as possible. Porous injectors delivered a uniform, one dimensional flow with little recirculation.

Injectors with small orifices parallel to the direction

of flow (showerhead design) were used to study the effects of deviations from the assumed uniform, one dimensional velocity profiles.

To create a strong recirculation pattern between the combustion zone and the injector for this experiment and thereby increase the heat transfer to the injector, a triplet type injector was designed.

From past experience with liquid rocket motor injectors, it was well known that a triplet configuration created high rates of heat transfer to the injector. Turbulence and high gas velocities in the combustion zone and across the face of the injector reduce the thickness of the boundary layer at the injector face and increase the transport of hot combustion gases from the combustion zone to the injector. Both of these effects greatly increase the heat transfer rate to the injector.

Maintaining the same total orifice area in the injector as was used in all preceding injectors with orifices, made the single triplet injector unusable because of combustion flashback into the mixing chamber.

The probability of flashback is related to the diameter of the orifice and the gas velocity through the orifice, therefore to reduce flashback, keeping the same total orifice area and roughly the same propellant mass flows, it was necessary to design a six orifice double triplet injector (Figure 4a).

This injector configuration was used throughout this experiment with a propellant combination of hydrogen and air (stoichiometric mixture ratio = 34.5) premixed in the mixing chamber upstream of the injector.

B.1 Procedure

Rocket motor length was varied from 1.625 to 40 inches for the experiment and at each test length a full traverse of equivalence ratios was made from the fuel lean flammability limit to the fuel rich flammability limit. A constant chamber pressure of 100 ± 2 psig was maintained. At each length, the equivalence ratios of the unstable region limits and frequencies and amplitudes of the instabilities were recorded. Unstable region limits were approached both from the stable and the unstable side of the limit.

After data were collected, propellant mass flows were corrected for temperature and gauge pressure error and the unstable regions were plotted on a graph of equivalence ratio versus motor length.

B.2 Results

Figure 7 compares the unstable regions and their limits found in this experiment using the six orifice double triplet injector with those regions found by previous investigators using the injectors described earlier.

B.3 Discussion

Past experiments using porous injectors (3) recorded

no unstable regions below a motor length of five inches and experiments using ceramic coated and water cooled injectors (4) did not test for instability below 5.5 inches.

Using the six orifice double triplet injector, high frequency, longitudinal instabilities were recorded down to a motor length of 2.5 inches. A new region of high frequency longitudinal instability was found on the fuel rich side of stoichiometric between 2.5 and seven inches and an extremely low frequency region (100-200 cps) was noted between 1.625 and two inches.

The new, high frequency, longitudinal instability region found between 2.5 and seven inches cannot be explained. Results using the six orifice double triplet injector almost paralleled the results of previous investigators except for this region and the low frequency region. The high frequencies in this region had the same acoustic frequencies for chambers of corresponding length but there was a distinct separation in equivalence ratio between the new region and the other regions found using the six orifice double triplet injector.

It is suspected that the low frequencies were not longitudinal instabilities since high frequencies are associated with the acoustic properties of short combustion chambers. At very short lengths, the chamber diameter is of the same order as the chamber length (~ 1.5 inches) and the pressure transducer diaphragm is partially covered by the inserted

nozzle (Figure 5). This chamber configuration could account for the presence of the non-longitudinal instabilities recorded.

A hysteresis effect on the fuel lean unstable region limit can be seen in Figure 7, with the arrows indicating whether the limit was approached from the stable or the unstable region. This effect was also noted at the fuel rich limit (not shown for sake of clarity) and amounted to a difference in equivalence ratio of 0.15 at both limits.

Proof that the double triplet configuration did greatly increase the heat transfer to the injector compared with other configurations was evidenced by mechanical deformation (warping) of the injector after a few runs. To preclude any change in the propellant injection pattern due to misalignment of the triplet injector orifices caused by the deformation, injectors were replaced whenever distortion was evident.

It was not possible to confine the upper limit of the unstable region on the fuel lean side of stoichiometric to a single value of equivalence ratio. At the lean mixture ratios of the upper limit (105 to 140 parts of air to one part of hydrogen) the amplitude of the instability was very small, making it difficult to detect exactly when unstable combustion stopped and stable combustion began. Therefore an envelope of equivalence ratios is shown on Figure 7 in which the unstable region limits were still found.

Notice from Figure 7 that beyond a length of 25 inches

the unstable region on the fuel rich side of stoichiometric terminates. This termination is attributed to the facts that as the combustion chamber length increases the combustion gases lose more and more heat to the walls of the chamber. This and damping effects associated with chamber length either eliminate the instability completely or reduce the amplitude of the instability to a value that is too small to be detected.

Reproducibility and reliability of data taken during runs with chamber lengths less than five inches is poor. Many factors contribute to these poor data. At short lengths the motor cannot be adequately cooled, causing the chamber temperature to vary with the length of the run. Also the propellants do not have sufficient time in the chamber to react to completion, before exiting through the nozzle, causing an unknown variation of the combustion gas composition.

Another factor would be an unknown, non-constant heat loss, due to surface and wall irregularities caused by holes cut in the steel liner to accommodate the pressure transducer and spark plug ignitors.

It is felt that data obtained at lengths below five inches should be viewed with caution if not discarded altogether. If these lengths do become of interest, redesign of this motor section should be accomplished.

The equivalence ratios which determined the unstable region limits under steady run conditions were reproducible within 2% at motor lengths tested between five and 40 inches. This variation was attributed to: human judgement in determining the exact time (and therefore equivalence ratio) of the onset of instability from transient pressure measurements in the combustion chamber displayed on an oscilloscope; the rate at which the equivalence ratio was changed by the technician; and the degree of roughness with which the propellant settings were altered. (Abrupt changes versus smooth changes of the propellant pressure regulators.)

C. Decreasing Heat Transfer Rate to Injector

To study the effects of decreasing the rate of heat transfer to the injector, the combustion zone was moved farther downstream from the injector than in the previous experiment.

In order to move the combustion zone downstream, it was necessary to modify the original configuration of the rocket motor by completely removing the mixing chamber with the injector fitted in the downstream end.

The impingement injector plate (Figure 2), through which unmixed propellants previously entered the mixing chamber in the unmodified configuration, was used in this experiment with an adaptor section, as the injector for the combustion chamber.

This change in injection scheme left a region of unmixed, unburned, relatively cool propellants to act as an insulator between the combustion zone and the injector, since the propellants required a finite distance from the injector plate to form a combustable mixture. Any recirculation of hot combustion gases had to pass through this cool region before contacting the injector face, thus reducing the heat transfer rate to the injector.

The hydrogen and air propellants were injected, unmixed through the injector plate directly into the combustion chamber where, when ignited, a chamber pressure of 100 ± 2 psig was

maintained.

C.1 Procedure

A full equivalence ratio traverse was made at a motor length of ten inches. As in the previous experiment, frequencies and amplitudes of the instabilities were recorded. The equivalence ratios at the limits of the unstable regions were corrected for temperature and gauge pressure error and compared with the results of the first experiment. All unstable region limits were approached from both the stable and the unstable side.

C.2 Results

The region of instability that was observed on the fuel lean side of stoichiometric had the same limit as that observed using the six orifice double triplet injector in the first experiment. A similar hysteresis effect on the limits was observed, depending upon whether the limit was approached from a region of stability or instability.

An exact upper limit of this region was difficult to determine, (for reasons stated in the first experiment) but it always fell within the same limiting envelope (Figure 7)

The fuel rich region of instability was bounded by the same limit as was found for the six orifice double triplet injector, but the flammability limit was found to be at a much richer fuel mixture, $\phi = 6.05$ compared to $\phi = 4.5$.

C.3 Discussion

It was apparent from the results, that the unstable regions and their limits were unaltered by a decrease in the heat transfer rate to the injector. Since the flammability limit for a given propellant combination has a certain value, the apparent change in the fuel rich flammability limit can be attributed to the fact that the gases were poorly mixed before entering the combustion zone. After combustion had occurred, an even greater excess of unburned hydrogen was present in the combustion products than was present when the propellants were premixed.

Examination of the impingement injector plate between and after runs, revealed no deformation or discoloration, which verified the fact that the heat transfer to the plate was far less than the heat transfer to the six orifice double triplet injector during the first experiment.

The reproducibility of data taken was good, with the same amount of scatter accountable to the same reasons stated in the first experiment.

D. Increasing Heat Transfer Properties of Combustion Gases

In this experiment the heat transport properties of the combustion gases were altered to study the effects of changing the heat transfer rate in the combustion chamber on previously found regions of combustion instability.

The heat transport properties, thermal conductivity, k , viscosity, μ , specific heat, c_p , and the density, ρ , were altered by changing the inert diluent in the oxidizer. In the preceding experiments, the combustion gases were formed by burning hydrogen and air as propellants. In this experiment, hydrogen was burned with a helium-oxygen mixture resulting in combustion gases containing helium instead of nitrogen.

It was felt that the helium present in the combustion products, having a greater thermal conductivity than nitrogen, would increase the heat transfer properties of the combustion gases, especially at equivalence ratios greater than one at which an excess of oxidizer is present in the combustion products.

The oxidizer used contained 80% of helium mixed with 20% of oxygen by volume with less than 1% deviation in either constituent according to the specifications of the gas company from which the gas was purchased.

The oxidizer had the following properties at STP conditions: molecular weight = 9.6, stoichiometric mixture

ratio when burned with hydrogen = 12, specific heat = 0.562 calories/gram °K and ratio of specific heats = 1.585.

A showerhead injector having ten orifices on two concentric circles (Figure 4b) was used to inject the premixed hydrogen fuel and helium-oxygen oxidizer into the combustion chamber. This injector had the same total orifice area as the six orifice double triplet injector.

D.1 Procedure

The motor length was varied in five inch increments between five and 30 inches and equivalence ratio traverses were made between the fuel rich and the fuel lean flammability limits while maintaining a chamber pressure of 100 ± 2 psig. As before, frequencies and amplitudes of the instabilities were recorded, and the unstable regions and their limits were plotted on a graph of equivalence ratio versus motor length. Each unstable region limit was approached from both the stable and the unstable side.

After the unstable region limits were determined experimentally, the adiabatic temperatures for the combustion reaction at the equivalence ratio of the limits were computed.

This calculation was made, assuming no dissociation at the temperatures of interest, by equating the heat of reaction to the enthalpy rise of the combustion products, water, helium, and excess oxygen or hydrogen, depending on the equivalence ratio of the limit.

For comparison, the adiabatic temperatures for the hydrogen-air reaction were computed at the equivalence ratios of the limits found in the first experiment (Chapter 111-B) assuming: no dissociation, and the composition of air to be 21% oxygen and 79% Nitrogen by volume. The results of these calculations are tabulated in Figure 9.

The heat transport properties of the combustion gases were calculated from the heat transport properties of each constituent in the combustion products, at the adiabatic temperatures and equivalence ratios of the experimentally determined unstable region limits.

The heat transport properties of the individual gases in the combustion products were gathered from existing literature on thermodynamic and heat transport properties of gases at high temperatures (6, 8, 10 through 15).

A heat transfer coefficient, h , was calculated at each experimentally determined unstable region limit from the heat transport properties of the combustion gases. This single property provided a better understanding and method for comparison of the differences in the heat transfer rates of the combustion gases and was calculated from a modified Chilton Colburn equation for turbulent flow in a duct:

$$h = \frac{a k}{d} \left(\frac{d v \rho}{\mu} \right)^{0.8} \left(\frac{c_p \mu}{k} \right)^{0.33}$$

Where d = diameter of combustion chamber, $a = 0.023$, and V = the velocity of the combustion gases in the combustion

chamber.

The heat transfer coefficients of the combustion gases at the unstable region limits found using both the air and helium-oxygen oxidizers are listed in Figure 9.

D.2 Results

Figure 8 shows the unstable regions and their limits found using the helium-oxygen oxidizer with hydrogen as a fuel when approached from the stable side of the limit, and also compares these limits with those found in the first experiment using the six orifice double triplet injector with air as an oxidizer.

Figure 9 is a tabulation of adiabatic combustion temperatures, heat transport properties and heat transfer coefficients computed for this experiment at the equivalence ratios of the unstable region limits found using both helium-oxygen and air oxidizers.

D.3 Discussion

It can be seen from figure 8 that altering the heat transport properties of the combustion gases did change the equivalence ratio at which the fuel lean unstable region limit was found compared with the limit found using air as an oxidizer.

The unstable regions are similar in form to the previously found regions, with the fuel lean region limit closest to stoichiometric occurring at a constant value of equivalence ratio and

the fuel rich region limit at a constant equivalence ratio for the first 20 inches of motor length. The limits (farthest from stoichiometric) of both unstable regions were found to be the flammability limits for the helium-oxygen propellant combination.

Because of the poor reproducibility and reliability of data mentioned earlier in this report, no runs were made below a motor length of five inches. Also the increased heat transfer coefficient of the combustion gases (Figure 9) made it impossible to cool the shorter chamber lengths without modifying existing cooling equipment.

A hysteresis effect on the unstable region limits of the same magnitude to that which occurred in the first two experiments was noted, but for clarity, only the limit determined when approaching from a stable region is shown in Figure 8.

It was not immediately apparent why the equivalence ratio of the fuel lean unstable region limit found using the helium-oxygen oxidizer was almost 20% greater than the limit found using air oxidizer, while the fuel rich unstable region limit was almost the same as the limit found using air oxidizer.

The adiabatic temperature calculated for the hydrogen and helium-oxygen reaction at the fuel rich limit was always found to be greater than the adiabatic temperature for the

hydrogen and air reaction. This fact is not obvious upon inspection of Figure 8, since the equivalence ratio of the hydrogen and air reaction decreases with increasing chamber length and the equivalence ratio for the hydrogen and helium-oxygen reaction is almost constant, the limits intersecting at a chamber length of 15 inches.

A careful examination and comparison of the adiabatic temperatures and the heat transfer coefficients calculated at all of the experimentally determined limits (Figure 9) revealed a significant trend.

The hydrogen and helium-oxygen reaction always produced the larger adiabatic temperatures at the limits of similar unstable regions. (Similar regions being regions of similar form on the same side of the stoichiometric equivalence ratio, found when using different oxidizers.) This reaction also produced the largest heat transfer coefficient at the same limits.

A comparison between the heat transfer coefficient at the fuel rich limit with the heat transfer coefficient at the fuel lean limit for either propellant combination, showed that the limit with the greater adiabatic temperature had the greater heat transfer coefficient.

A graph of heat transfer coefficients versus adiabatic temperatures calculated at all of the unstable region limits, found using both oxidizers, revealed an almost linear

relationship between increasing heat transfer coefficient and increasing adiabatic temperature.

The trend of the larger heat transfer coefficients being associated with the larger adiabatic temperatures led to speculation about the actual temperature of the gases in the combustion chamber at the unstable region limits.

It was postulated that the combustion gas temperatures in the chamber were the same at the limits of all of the unstable regions, regardless of equivalence ratio or propellant combination. To test the validity of this argument, the next experiment (Chapter III-E) was performed to measure the maximum temperature in the combustion chamber when hydrogen was burned with both air and helium-oxygen oxidizers.

The reproducibility and accuracy of this experiment was affected by two problems: the inability to acquire an oxidizer mixture with constant composition throughout the total volume of the gas, and the inability to accurately calibrate critical flow orifices.

It was possible to eliminate the errors introduced by these problems by following precise, although time consuming, experimental procedures.

Analysis showed that an error of 7% in the equivalence ratio could be expected, if the oxygen content of the oxidizer varied as much as $\pm 3\%$ during a run. This possible error was minimized by carefully measuring the oxygen content of

the oxidizer before and after each run to estimate an average oxygen content during the run for calculating equivalence ratios and the mole fractions of products in the combustion gases.

Although the oxidizer specifications cited a 1% deviation of either constituent in the 80% helium-20% oxygen oxidizer, the oxygen content of the gas mixture delivered by the supplier, varied between 17 and 23%. This measurement was made with a Beckman oxygen analyzer.

The uncalibrated orifice was used only during some runs at equivalence ratios less than one, and less than a 4% error in equivalence ratio was expected when using the uncalibrated orifice. This error can be completely eliminated from all data, when an accurate calibration is made to establish the discharge coefficient of the orifice.

This problem arose when smaller orifices were manufactured for the oxidizer metering system, and no method was available to calibrate them. Calibration of the existing orifices was originally done by Pelmas (3), using a specially built device. Since the device was quite large, it was dismantled after all orifices had been calibrated.

His calculations showed calibrated orifices of the same design to have a discharge coefficient of 0.97 for upstream pressures between 500 and 1300 psig. For lack of a better method, ideal mass flow calculations were used for the

uncalibrated orifices corrected by a discharge coefficient of 0.97.

To check the actual mass flow through the uncalibrated orifices (even though a crude check), a run in a stable region was made at a constant chamber pressure and constant fuel flow, noting the oxidizer mass flow through a calibrated orifice. Then the conditions were duplicated using an uncalibrated orifice and the mass flow through this orifice was assumed to be the same as through the known orifice. The data points that were established by this method were within $\pm 2\%$ of the ideal mass flows corrected by the discharge coefficient.

E. Combustion Gas Temperature at Unstable Region Limits

This experiment was performed to measure the maximum combustion chamber temperatures at the experimentally determined unstable region limits found in the previous experiments when hydrogen and air and hydrogen and helium-oxygen oxidizers were burned in the gas rocket motor.

E.1 Procedure

The unstable region limits were found by experiment in Chapter III-B and III-D using different injectors and oxidizers. In this experiment, temperature measurements were made with both injector configurations (Figure 4) and both air and helium-oxygen oxidizers.

All test runs were made at a length of 15 inches, maintaining a chamber pressure of 100 ± 2 psig. This length was chosen because the fuel rich unstable region limits found using both oxidizers occurred at the same equivalence ratio. The propellants were premixed in the mixing chamber before being injected into the combustion chamber.

Five 0.062 inch diameter platinum-platinum plus 10% rhodium thermocouples with stainless steel shields were installed in the combustion chamber to measure the temperatures along the longitudinal axis of the combustion chamber (Figure 10).

The thermocouples were originally positioned 0.75, 1.5, 2.5, 3.5, 4.5 inches from the face of the injector. Later

in the experiment the thermocouple located at 4.5 inches was removed and was placed 1.125 inches from the injector, to give a more detailed temperature description of the combustion zone close to the injector.

The initial tests were made on the stable side of the fuel rich unstable region limit to preclude possible oxidation of the stainless steel thermocouple shields.

It was suspected that the thermocouples would be destroyed by oxidation when running the motor on the fuel lean side of stoichiometric, because of the high temperatures and the presence of excess oxygen in the combustion products.

Later, runs using thermocouples with 0.002 inch rhodium plating on the stainless steel shield were made on the fuel lean side of stoichiometric. As suspected, the thermocouple shields were completely oxidized away before steady run conditions could be established and before any data could be taken (less than 10 seconds).

The exact limit of the unstable region was first determined with the thermocouples removed from the motor and the holes pressure capped and then the run was duplicated with the thermocouples in place. In this manner run time was held to less than 20 seconds, which prevented deterioration of the thin thermocouple shields from the high temperatures in the combustion chamber.

After each run, each thermocouple was inspected for

7

condition and replaced if it appeared discolored or deformed, and the temperature recorded at that thermocouple was reviewed for any error caused by the deterioration of the thermocouple.

Temperatures at each thermocouple were recorded measuring from the injector downstream and back again to confirm the accuracy of the first readings after a time delay. Each thermocouple was interrogated for one second by means of a thermocouple selector switch (Chapter 11-G).

Thermocouple readings were taken ten seconds after the motor had been started, at which time the thermocouples were at a steady value of temperature. A full set of thermocouple readings were taken at the fuel rich limit of the unstable region for each injector using both the helium-oxygen and air oxidizers.

E.2 Results

Figure 11 shows the combustion chamber temperature profiles measured downstream of the six orifice double triplet injector (a), and the ten orifice injector (b). Temperatures were measured on the stable side of the fuel rich unstable region limit when burning both the air and the helium-oxygen oxidizers with hydrogen fuel.

E.3 Discussion

The maximum temperatures measured on the stable side of the fuel rich unstable region limits for each propellant

combination differed by only 40°C , with the highest temperatures always recorded when burning the hydrogen and helium-oxygen propellants.

When the propellants entered the combustion chamber through the ten orifice injector, higher maximum temperatures were measured than when they entered through the six orifice double triplet injector. The difference in maximum measured temperatures was attributed to the strong recirculation pattern caused by the double triplet injector compared to the ten orifice injector. This strong recirculation pattern is known to increase the heat transfer rates to both the injector and walls of the combustion chamber, therefore decreasing the maximum temperature in the chamber.

An analysis of the radiative heat losses (16) from the thermocouples to the chamber walls, indicated that a thermocouple would never read more than 40°C below the actual temperature of the combustion gases formed by the hydrogen and air reaction, and never more than 20°C below the actual temperature of the combustion gases formed by the hydrogen and helium-oxygen reaction.

This analysis showed that the maximum differences between measured and actual temperatures occur when the difference between thermocouple and wall temperature is over 500°C . Any difference less than 500°C , and the thermocouple corrections are less than the maximum but still in the ratio of two to one.

With radiative heat loss corrections applied to the measured temperatures, the actual temperatures in the combustion chamber for different propellant combinations differed by less than 40°C . At the temperatures being measured, this amounted to less than a 4% difference and tended to confirm the postulate that the unstable region limits do indeed occur at the same combustion chamber temperature.

No temperature data were recorded at the fuel lean unstable region limits due to the rapid destruction of the thermocouples by oxidation. Further temperature investigation must be carried out at these limits, using a different scheme of temperature measurement, not affected by oxidation, to determine whether the postulate of equal temperatures at all unstable region limits, regardless of equivalence ratio or propellant combination is valid.

The temperature profiles in Figure 11 clearly define a distance from the injector face to a point of maximum combustion chamber temperature, or a reaction zone, in which the combustion reaction had reached completion. The distance to the point of maximum temperature was dependent upon only the injector configuration and not upon the propellant combination being burned in the chamber.

The presence of this reaction zone confirmed the assumption made by Crocco and Bortzmeyer (2) and Sirignano (17), that the reaction zone was very small compared to the

length of the combustion chamber except for the very small chamber lengths.

Using the same propellant combination, higher temperatures were measured by the thermocouple 0.75 inches from the six orifice double triplet injector face than the same distance from the ten orifice showerhead injector face. This further confirmed the observation in Chapter III-B, that the triplet injector configuration does increase the transport rate of hot gases from the combustion zone to the injector face.

Temperature measurements taken at the same thermocouple location during separate runs, using the same oxidizer and injector, and at the same equivalence ratio, were reproducible within 5°C .

It must be noted that the adiabatic combustion temperatures calculated in this temperature range ($1350\text{-}1450^{\circ}\text{C}$) vary about 3.5°C with a change in 0.001 in the equivalence ratio. From this it can be seen what magnitude of temperature error might result from the inability to determine the equivalence ratio to three decimal places and any unknown oxidizer composition change during the run.

F. Effect of Chamber Pressure Variation

Throughout the first four experiments, any effect of chamber pressure variation on the unstable regions and their limits was eliminated by maintaining a constant chamber pressure of 100 ± 2 psig during all runs. In this experiment, the chamber pressure was maintained constant at 50 and 150 psig and effects on the unstable regions noted.

F.1 Procedure

Complete equivalence ratio traverses were made at ten and 20 inch motor lengths and constant chamber pressures of 50 and 150 psig using hydrogen and air as propellants and the ten orifice showerhead injector.

The equivalence ratios at the limits of the unstable regions, corrected for temperature and gauge pressure error, and the frequencies and amplitudes of the pressure oscillations in these regions were recorded.

F.2 Results

No changes in the limits of the unstable regions were noted when data at 50 psig and 150 psig chamber pressures were compared. A further comparison of data with the unstable regions and limits found in the first experiment (using the six orifice double triplet, hydrogen and air, and 100 psig chamber pressure) revealed no change in the equivalence ratios at which the unstable regions occurred.

When an unstable region was entered by varying the

equivalence ratio, the chamber pressure would decrease. This pressure decrease was caused by the increased rates of heat transfer to the combustion chamber walls, caused by the instabilities, and resulted in a decrease in the combustion gas temperature in the chamber.

When a traverse of the unstable region was made, the mean chamber pressure was maintained constant by increasing the total mass flow of propellants in the desired equivalence ratio.

When leaving an unstable region at a constant chamber pressure, a hysteresis effect on the region limits was noticed. This effect had the same magnitude as noted in previous experiments in this report.

The frequencies of chamber pressure oscillations, recorded at the limits of the unstable regions during this experiment, at 50 and 150 psig, were compared with the frequencies recorded at the same equivalence ratios in the first experiment at 100 psig.

This comparison revealed frequency variations no greater than 5% between the frequencies found at the experimentally determined limits at all chamber pressures. The scatter can be attributed to a change in the speed of sound in the combustion chamber caused by a small variation in equivalence ratios between comparative runs.

G. Wave Form of Unstable Oscillations

Early in 1963, a shock wave theory based on a simplified model for combustion instability was proposed at Princeton University (17) predicting a definite relationship between the form of the oscillatory wave in the unstable combustion chamber of a premixed, gaseous propellant rocket motor, and the type of driving force maintaining the instability.

The following experiment was performed to determine the pressure versus time wave form of the instabilities in the combustion chamber so that they could be analysed in light of the proposed theory.

The fundamental frequencies of the instabilities were of the same magnitude as the acoustic frequencies associated with the chamber length and temperature, and when burning hydrogen and air, were less than 1500 cycles per second for chamber lengths greater than ten inches.

The wave forms of the instabilities were measured at different distances downstream from the injector face with a Dynisco PT49 pressure transducer, with the pressure sensitive diaphragm (diameter = 0.689 inches) mounted flush with the inner combustion chamber wall.

The frequency, amplitude and wave form of the instability were displayed on a Tektronix Type 535, single beam oscilloscope, and recorded with a Polaroid camera attached to the oscilloscope.

The Dynisco transducer had a reasonably flat output/ input response up to ten kilocycles, with a natural frequency of 22 kilocycles. Low pass filters were used to suppress the natural frequency of the transducer without suppressing the higher harmonics of the instabilities being measured.

All runs were made using the ten orifice injector with hydrogen and air propellants which were premixed in the mixing chamber before injection into the combustion chamber.

G.1 Procedure

In order to find out at what length and transducer position the best wave form could be observed, unstable runs were made and photographed at varying chamber lengths, transducer locations, equivalence ratios, low pass filter values and chamber pressures.

Because of the basic design of the motor sections, and the locations at which a pressure transducer could be mounted, the length of 25 inches was chosen after all desired results were considered. At 25 inches, the transducer could be mounted at 1.625 inches from the injector, 1.5 inches from the nozzle entrance and exactly in the middle of the chamber without any equipment modification. This is the only length at which such symmetry of transducer location could be achieved.

After initial runs indicated that the amplitude of the instabilities were too small to produce greater than

0.1 and 1.2 millivolts of signal from the Dynisco transducer, the excitation voltage to the transducer was doubled, which in turn, doubled the output signal. With an excitation voltage of 20 volts, the Dynisco had a slope of 0.08674 millivolts per psi.

Before photographing the wave form, the unstable region was entered and traversed by varying the equivalence ratio and maintaining a predetermined constant chamber pressure until the highest wave amplitude was observed. The oscilloscope was then set for single sweep operation and triggered manually to record a one sweep trace on the film.

G.2 Results

Figure 11 shows Polaroid pictures of unstable combustion wave forms recorded with the Dynisco transducer at three different locations in the chamber, a 25 inch combustion chamber length, equivalence ratio = 2.54 and chamber pressure = 100 psig. The ten orifice injector was used with hydrogen and air propellants.

G.3 Discussion:

A definite shock wave form was evident in all pictures (Figure 11) from the initial steep rise and the gradual decay of pressure as the wave passed across the transducer face.

Two unsymmetrical pressure rises within the period of oscillation will be noted in Figure 11a and 11b, when

the transducer was located close to the ends of the chamber. The initial steep pressure rise with only a short decay time, was followed by another steep pressure rise and a long gradual decay as the wave, reflected from the end of the chamber, passed across the transducer again.

The wave form of the shock measured at the center of the chamber (Figure 11c) had two symmetrical pressure rises within the period of oscillation and the amplitude measured was almost one half of the amplitude measured at the ends of the chamber.

The general wave form of the instabilities measured at different locations, agreed with the expected form of a shock wave oscillating at the acoustic frequency of the chamber, but the recorded form of the wave was unacceptable for purposes of analysis.

Using the Dynisco transducer, the wave form appeared to change during the run, while the frequency and amplitude remained constant. This, and the presence of high frequencies superimposed on the fundamental frequency, made it impossible to analyze the slope of the decaying portion of the wave.

It was felt that further experiments should be performed to determine the relationship between a smaller pressure sensing diaphragm diameter and the reproducibility of wave form. Since in the limiting case, a transducer with a sensing element diameter approaching zero, would give the

most accurate pressure description of the passage of a shock wave. Also with better frequency filtering, the high frequencies superimposed on the fundamental frequency could be eliminated without disturbing the true wave form and a detailed mathematical analysis of the wave could be performed.

CONCLUSIONS

Experiments indicated that the model chosen to describe the driving mechanism of the instability in the theory proposed by Crocco and Bortzmeyer (2), ie: an oscillating heat transfer to the injector plug coupled with a pressure oscillation in the combustion chamber, is not a valid model for this rocket motor. This theory predicted the presence of instabilities as a function of a dimensionless heat transfer coefficient, $\bar{h} = \frac{h^*}{\dot{m}^* C_p}$, a function of the dimensional heat transfer coefficient, h^* , at the injector surface, specific heat, C_p , and mass flow rate, \dot{m}^* . In the theory, the onset of instability was found to be sensitive to small changes in \bar{h} , (Reference 2, Figures 3 and 4).

Experimental evidence in this report showed that large changes in the heat transfer rate to the injector did not affect the occurrence of instability, the equivalence ratio limits which bordered the regions of instability, or the frequency of the instability.

A detailed analysis of the heat transport properties of the product gases found at the experimentally determined unstable region limits indicated an almost linear relationship between a rising heat transfer coefficient and a rising adiabatic combustion temperature. This observation led to further consideration of a postulate (3) that, the unstable

region limits encountered when using different propellant combinations in the gas rocket motor, occurred at the same actual combustion chamber temperature.

The early experiments of Bertrand (4) were concerned with the similarity at the unstable region limits of the adiabatic temperatures of combustion and the temperatures measured by one thermocouple located 3.75 inches downstream of the injector. These experiments left large discrepancies between the postulated similar temperatures and the measured temperatures, because, as determined in this report, the thermocouple was not measuring comparable temperatures in the reaction zone.

Experiments were carried out with a greater accuracy for further verification of the postulate that equal temperatures existed at the experimentally determined limits.

Experimental difficulties prevented temperature comparisons at the fuel lean region limits, but a comparison of the actual combustion temperature at the fuel rich limit revealed less than a 40°C difference in the combustion temperatures.

A definite reaction zone was measured in the combustion chamber, indicating that the combustion reaction had reached completion in a distance less than 1.5 inches downstream

of the injector face.

It was also shown that large changes in the combustion chamber pressure had no effect on regions of instability and their limits found during the experiments performed.

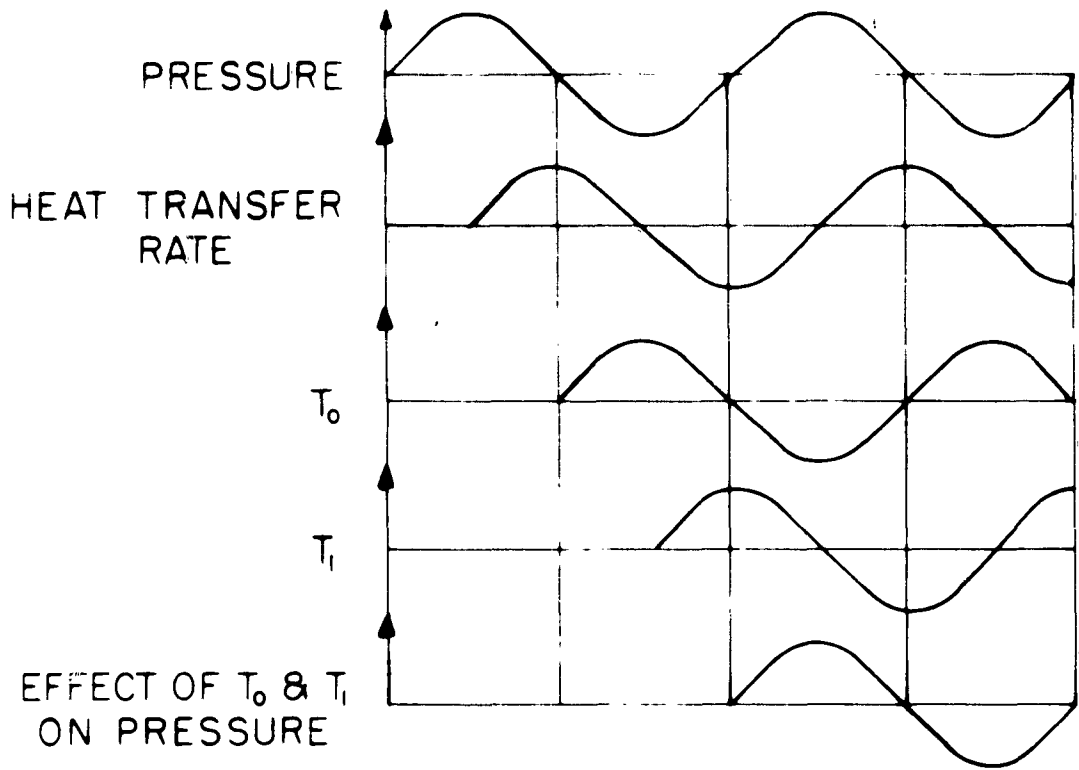
Finally, it was experimentally determined that the harmonic pressure oscillations in the combustion chamber were shock waves travelling at the acoustic frequency of the chamber. This result would appear to lend some credence to the shock wave model chosen in Reference 17.

It is felt that further experiments must be performed to explore more deeply the unstable region limit dependence on the actual combustion chamber temperature regardless of propellants, and the new consequences of the shock wave model for combustion instability.

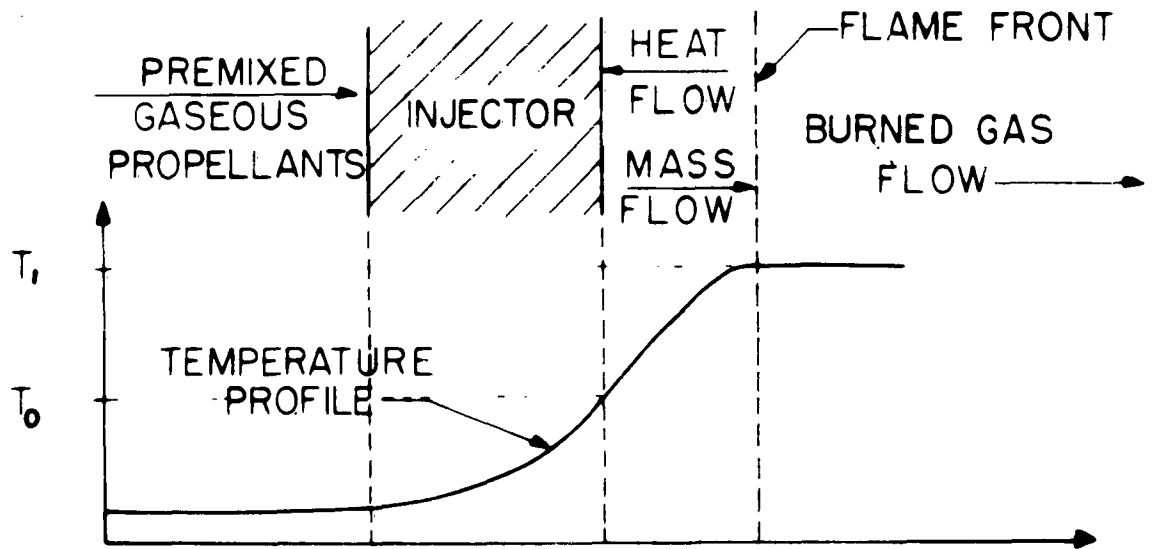
REFERENCES

1. Crocco, L. and Cheng, S.I., "Theory of Combustion Instability in Liquid Propellant Rocket Motors". Butterworth's Scientific Publications, 1956.
2. Bortzmeyer, H.G., "Analysis of Longitudinal High Frequency Combustion Instability in a Gas Fueled Rocket Motor". Aeronautical Engineering Laboratory Report No. 587, Princeton University, 1961.
3. Pelmas, R., Glassman, I., and Webb, M., "An Experimental Investigation of Longitudinal Combustion Instability in a Rocket Motor Using Premixed Gaseous Propellants". Aeronautical Engineering Laboratory Report No. 599, Princeton University, 1961.
4. Bertrand, J., "Theoretical and Experimental Investigations of Longitudinal High Frequency Combustion Instability in a Gas Fueled Rocket Motor". Aeronautical Engineering Laboratory Report No. 624, Princeton University, 1962.
5. Coward, H.F. and Jones, G.W., "Limits of Flammability of Gases and Vapors". U.S. Bureau of Mines, Bulletin 503, 1952.
6. Shapiro, A.H., "The Dynamics and Thermodynamics of Compressible Fluid Flow". (Volume 1), The Ronald Press Company, New York, 1953.
7. Barrere, M., Jaumotte, A., DeVeubeke, B., Vandenberg, J., "Rocket Propulsion". Elsevier Publishing Company, 1960
8. JANAF Thermochemical Data, The Dow Chemical Company, Midland, Michigan.
9. Sutton, G.P., "Rocket Propulsion Elements". John Wiley and Sons, Inc., 2nd Edition, 1958.
10. Woolley, H.W., "Thermodynamic Properties of Gaseous Nitrogen", NASA TN 3271, March 1956.
11. Eckert, E.R., Ibele, W.E., and Irvine, T.F., "Prandtl Number, Thermal Conductivity, and Viscosity of Air Helium Mixtures". NASA TND 533, September 1960.
12. Grier, N.T., "Calculation of Transport Properties of Heat Transfer Parameters of Dissociating Hydrogen". NASA TND 1406, October 1962.

13. Fano, L., Hubbell, J.H., and Beckett, C.W., "Compressibility, Density, Enthalpy, Entropy, Free Energy, Specific Heat, Viscosity and Thermal Conductivity of Steam". National Bureau of Standards Report 2335, June 1953.
14. Brewer, J., "Thermodynamic Data on Oxygen and Nitrogen". Technical Documentary Report Number ASD TR 61 625, September 1961.
15. Lemmon, A.W., Daniels, D.J., Sparrow, D.E., "Empirical Evaluation of the Properties of Steam at Elevated Temperatures and Pressures". Atomic Energy Commission, BMI 858, August 1953.
16. McAdams, W.H., "Heat Transmission". McGraw-Hill, Third Edition, 1954.
17. Sirignano, W., "Non-linear Aspects of Combustion Instability in Liquid Propellant Rocket Motors". Appendix F, Aeronautical Engineering Laboratory Report No. 553c, Princeton University, June 1963.



EFFECT OF T_0 & T_1 ON PRESSURE

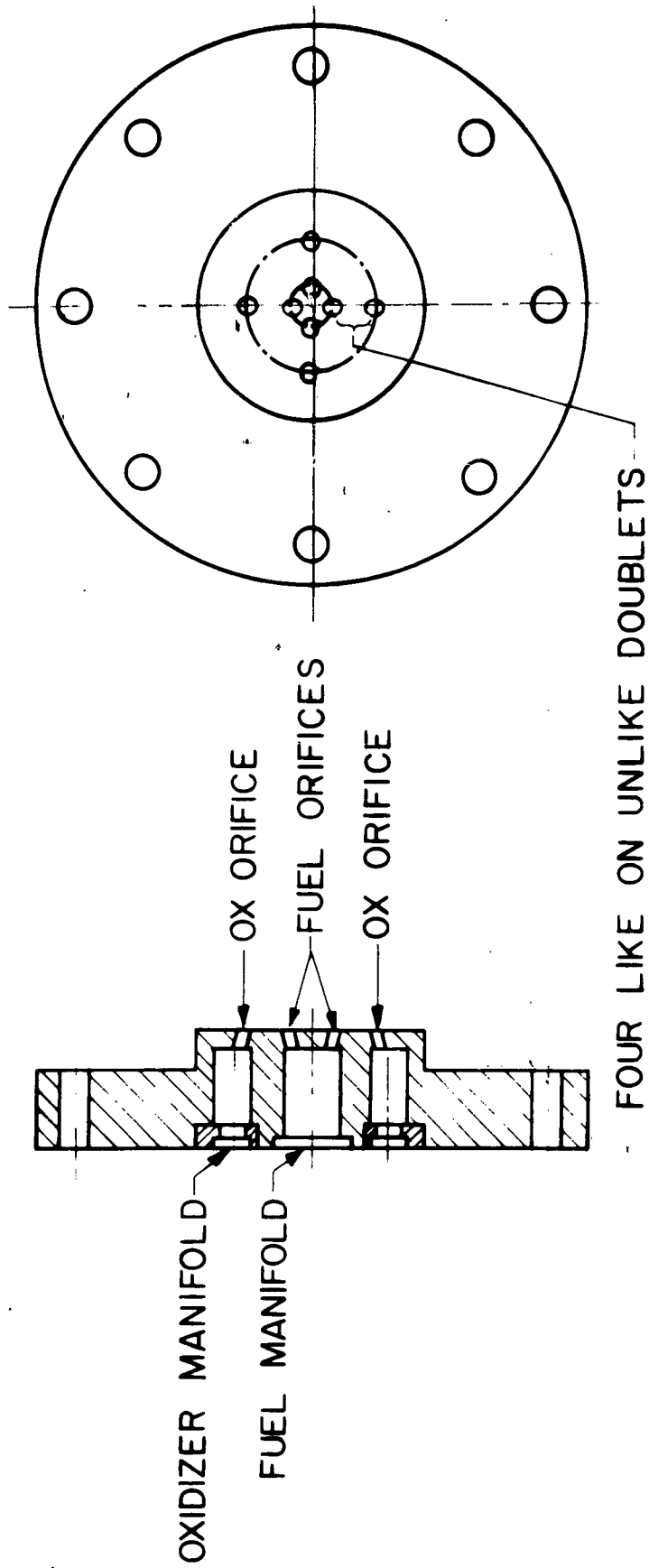


SCHMATIC OF OSCILLATING HEAT TRANSFER MECHANISM

FIGURE 1

JPL 1084

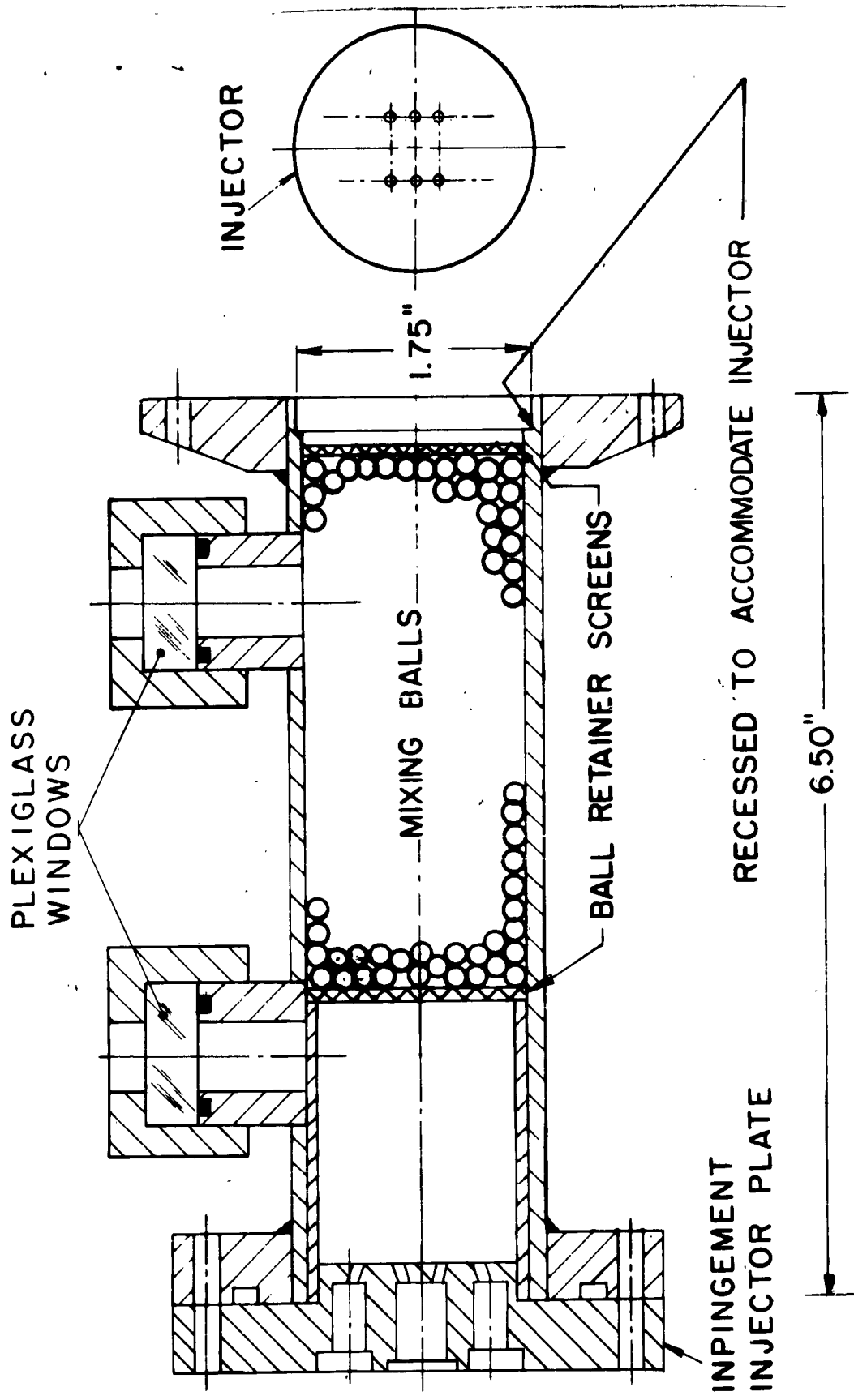
JPE 1662



IMPINGEMENT INJECTOR PLATE

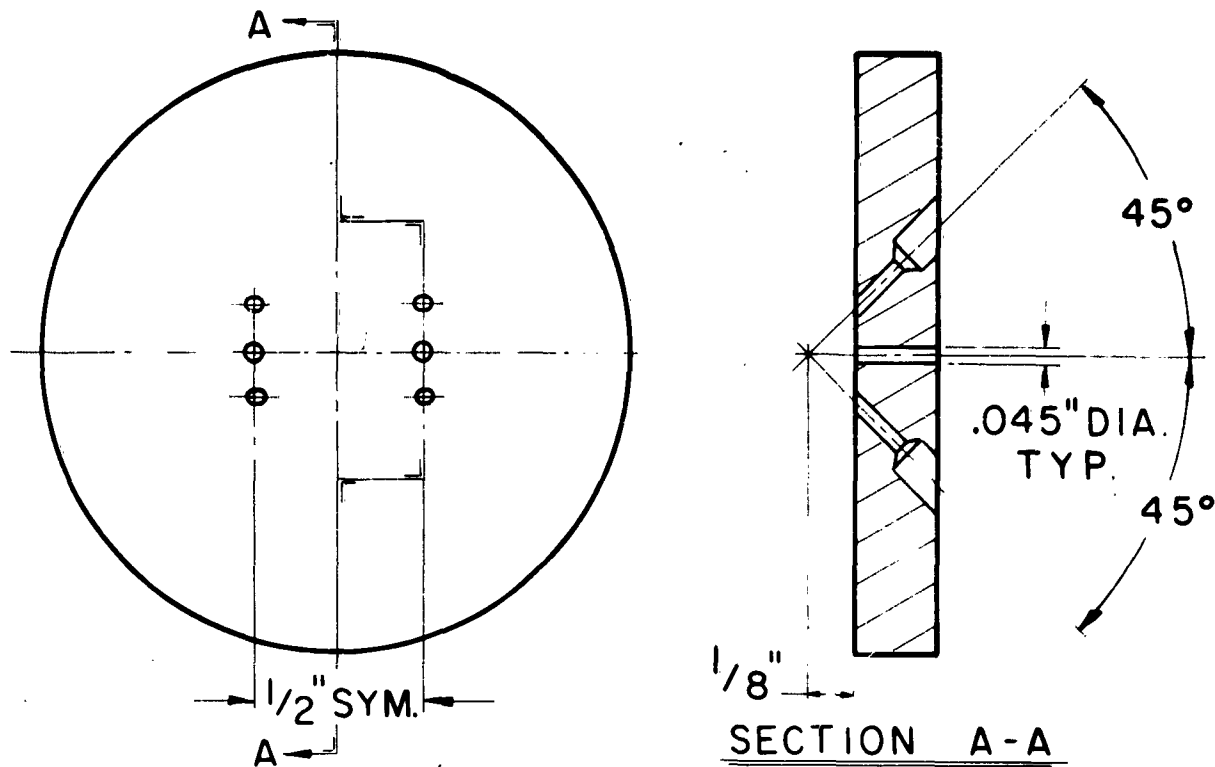
FIGURE 2

JPR 1669

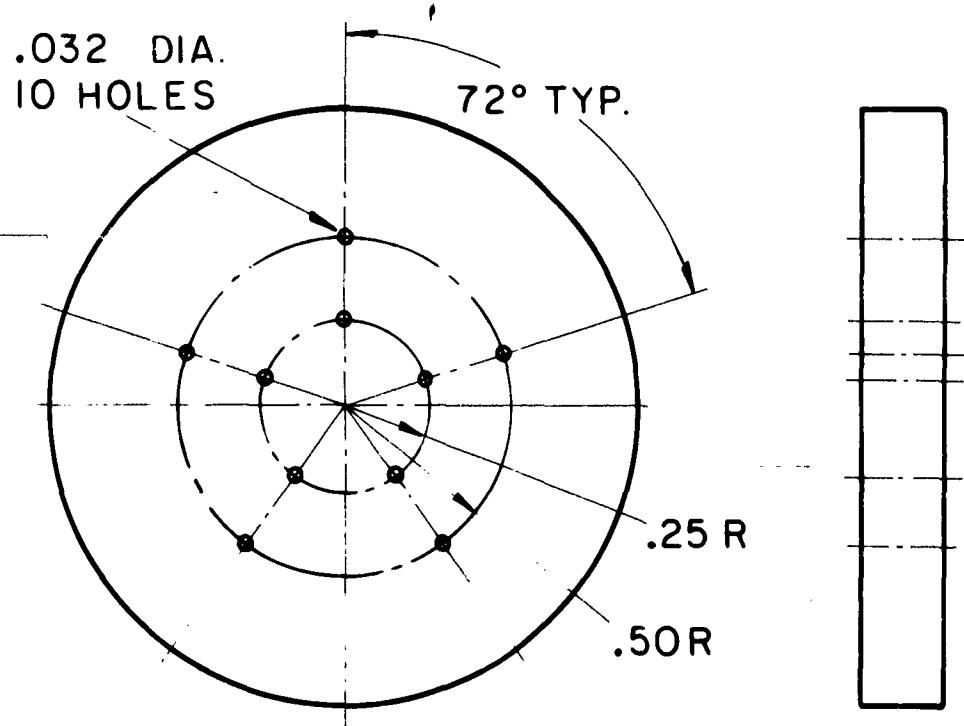


MIXING CHAMBER SECTION

FIGURE 3



a - SIX ORIFICE DOUBLE TRIPLET

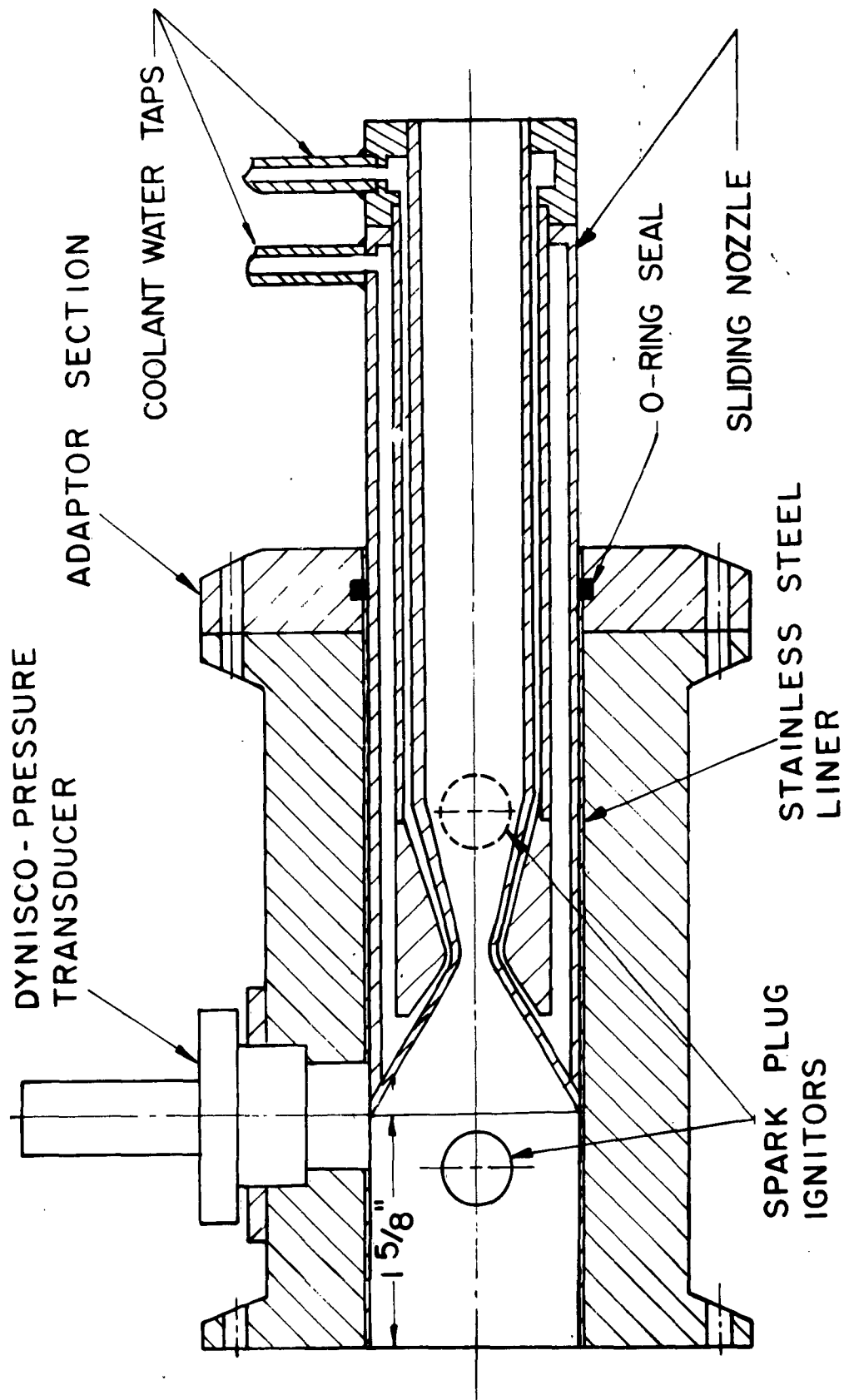


b - TEN ORIFICE SHOWERHEAD

INJECTORS

FIGURE 4

REF 1661



FIRST SECTION OF COMBUSTION CHAMBER
WITH NOZZLE INSERTED

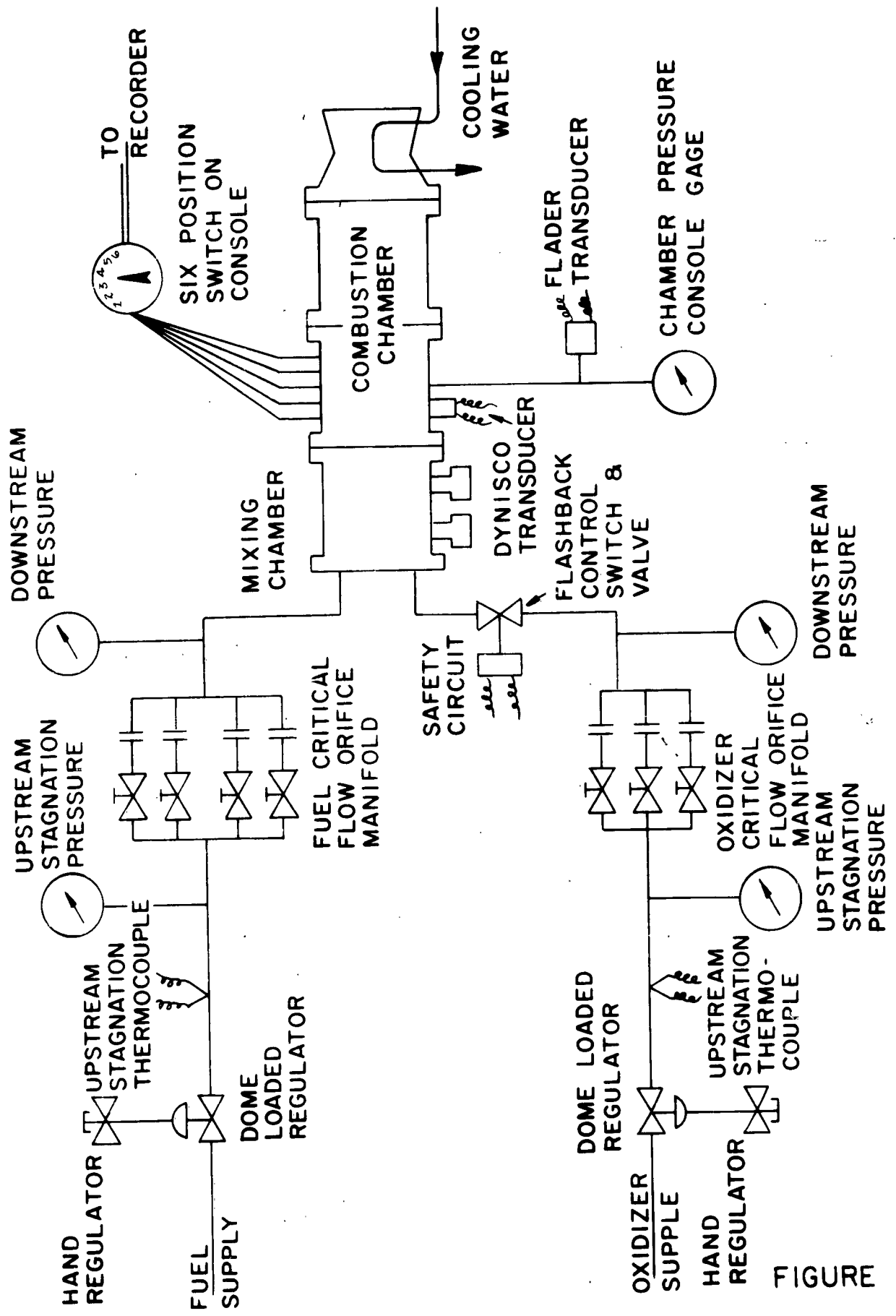
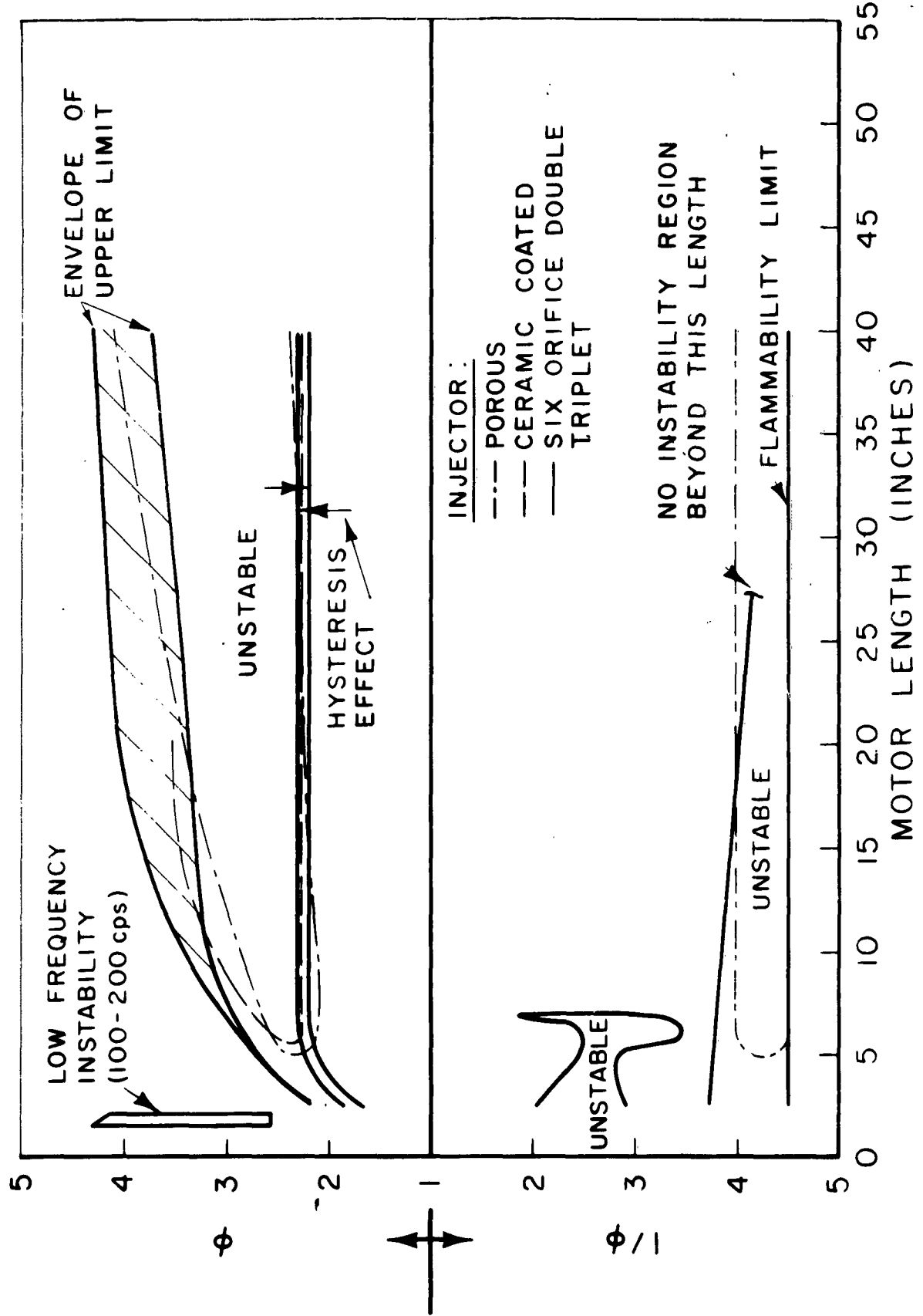
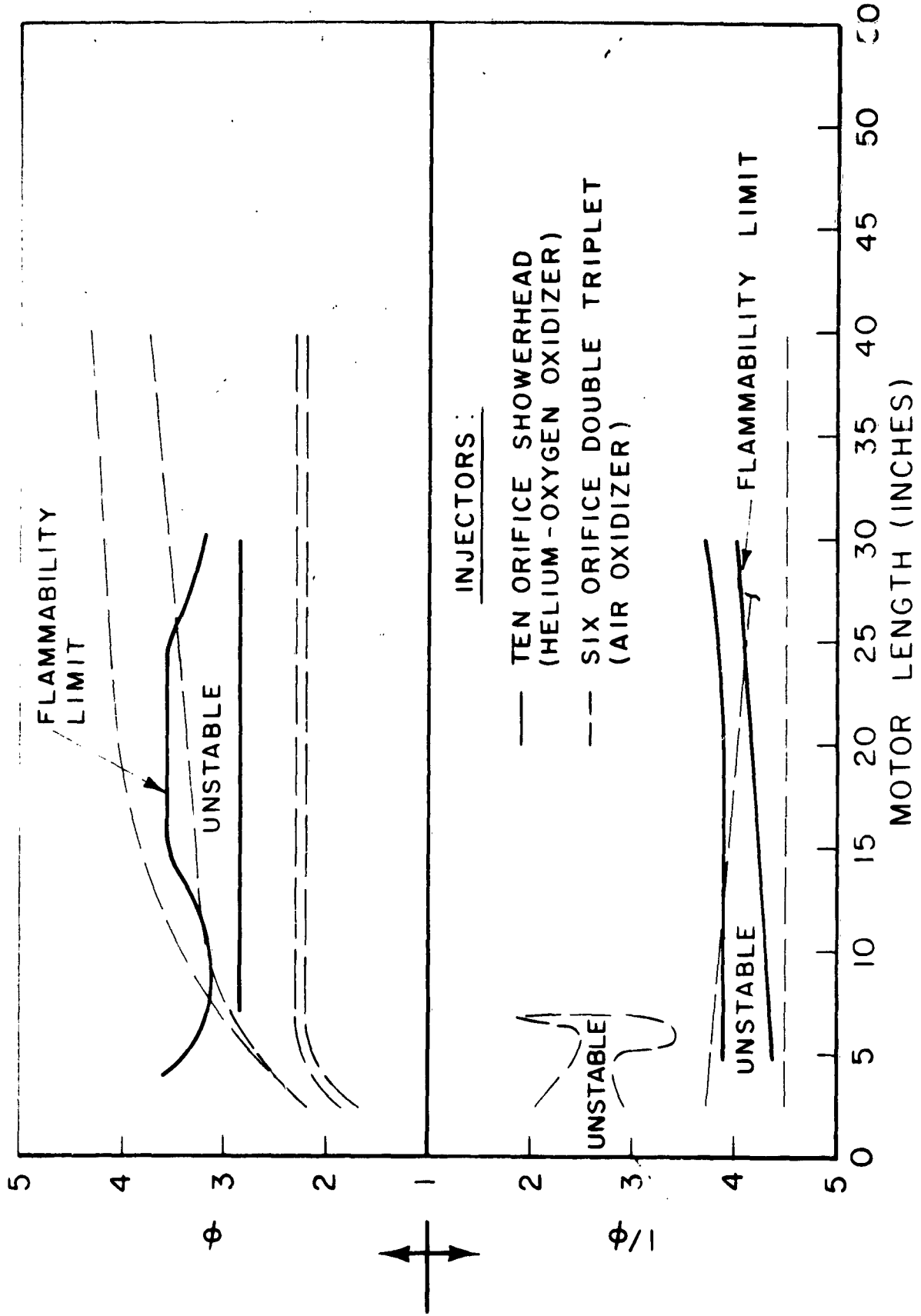


FIGURE 6



HYDROGEN FUEL AND AIR OXIDIZER

FIGURE 7



HYDROGEN FUEL AND HELIUM-OXYGEN OXIDIZER

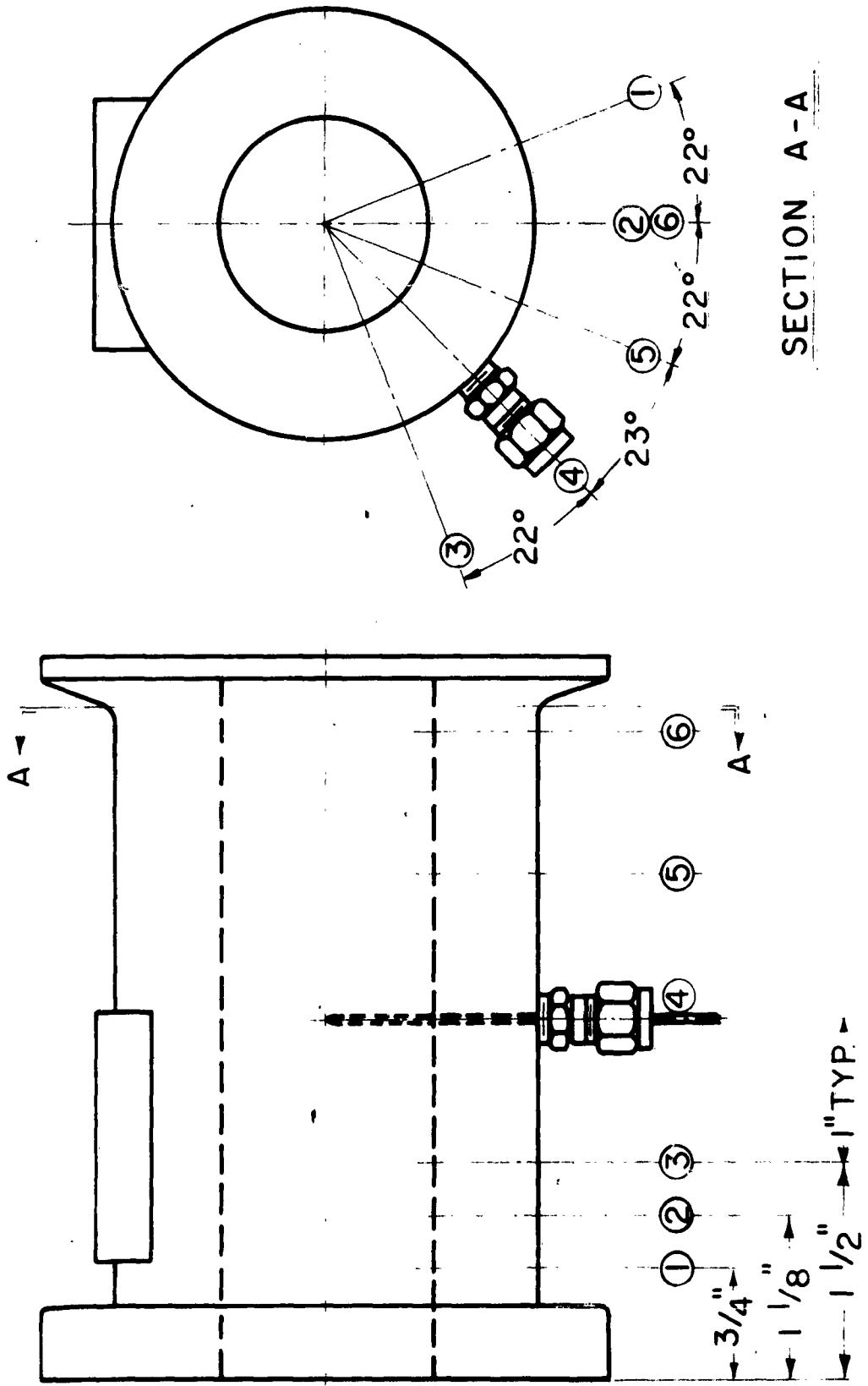
FIGURE 8

JPR 1677

| Oxidizer Used | Unstable Region | ϕ | T_{ad} °K | C_p cal / gm °K | ρ gm / cm ³ | k cal / cm sec °K | μ Poise | $P_{r.33}$ | R_{ev} °K | \dot{m} gm / sec | V cm / sec | \dot{m}^* cal / cm sec °K | T_{ch} °K |
|---------------|-----------------|--------|----------------|----------------------|--------------------------------|------------------------|----------------|------------|----------------|-----------------------|-----------------|--------------------------------|----------------|
| Air | Fuel Rich | .270 | 1625 | 2.10 | .838 | 8.44 | 4.06 | .935 | 1980 | 15.9 | 1.66 | 94.5 | 2.83 |
| | Fuel Lean | 2.33 | 1490 | .347 | 1.60 | 2.10 | 3.16 | .942 | 2000 | 21.0 | 1.16 | 24.0 | 3.29 |
| Helium Oxygen | Fuel Rich | .270 | 1725 | 2.46 | .361 | 17.2 | 4.47 | .914 | 1220 | 9.7 | 2.35 | 116.0 | 4.86 |
| | Fuel Lean | 2.83 | 1575 | 1.05 | .547 | 8.64 | 3.88 | .911 | 1320 | 14.1 | 2.25 | 62.5 | 4.22 |

$A_{chamber} = 11.45 \text{ cm}^2$
 $u_{chamber} = 3.32 \text{ cm.}$
 $V_{chamber} = \frac{\dot{m}^*}{\rho} A_{ch}$
 $Re_v = \frac{d_{ch} V_{ch} \rho}{\mu}$

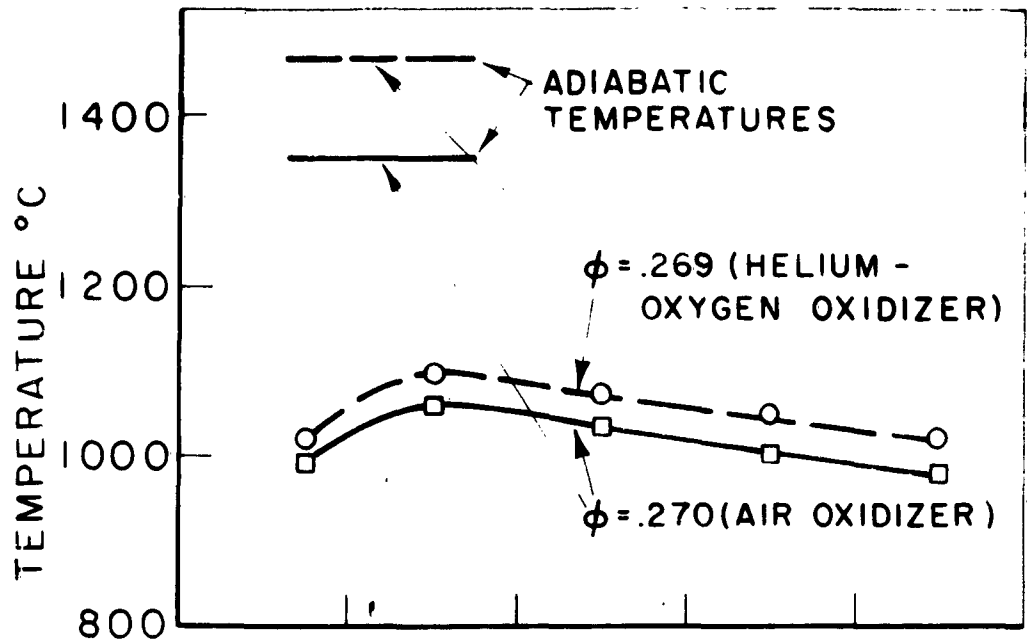
FIGURE 6



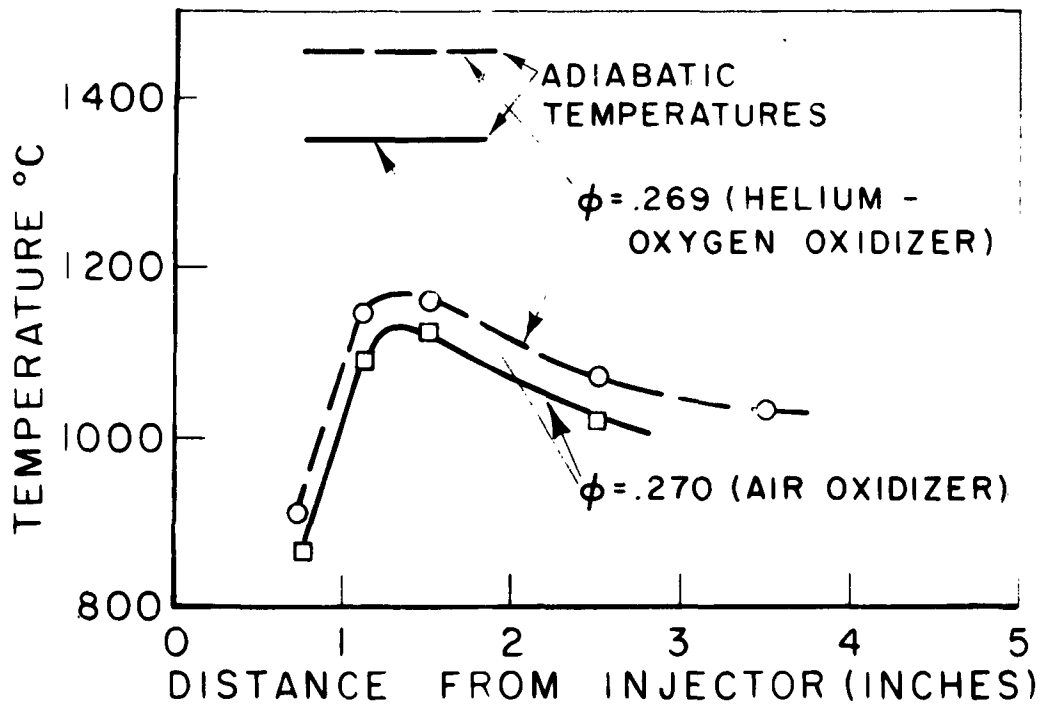
SECTION A-A

THERMOCOUPLE INSTALLATION IN COMBUSTION CHAMBER

FIGURE 10



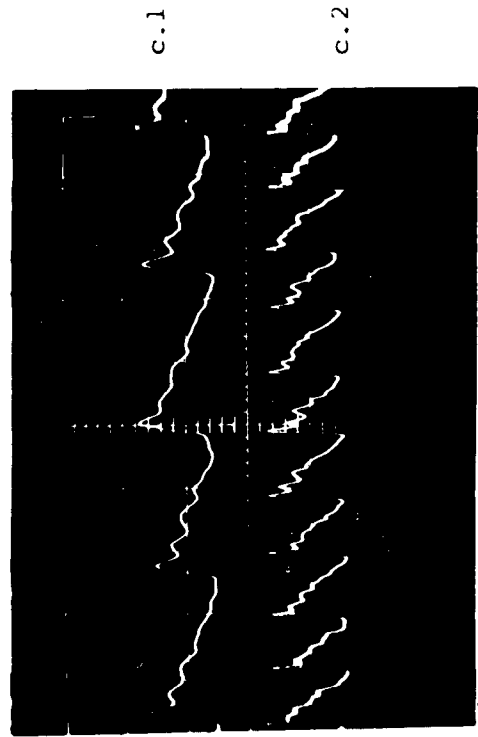
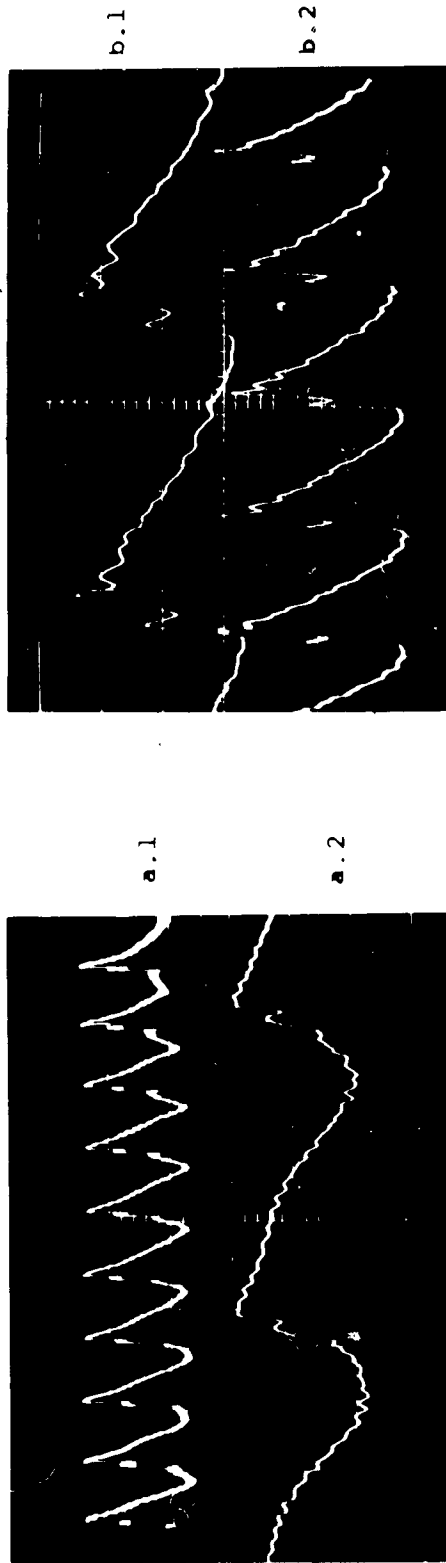
a - SIX ORIFICE DOUBLE TRIPLET INJECTOR



b - TEN ORIFICE INJECTOR

MEASURED AXIAL TEMPERATURE PROFILES
THROUGH COMBUSTION ZONE

JPR 1666



| Location | Distance from Injector [inches] | Amplitude Scale $\frac{\text{psi}}{\text{cm}}$ | Time Scale $\frac{\text{milliseconds}}{\text{cm}}$ |
|----------|---------------------------------|--|--|
| a.1 | 1.625 | 11.52 | 0.4 |
| a.2 | | | 2.0 |
| b.1 | 23.5 | 11.52 | 0.4 |
| b.2 | | | 1.0 |
| c.1 | 12.5 | 11.52 | 0.4 |
| c.2 | | | 1.0 |

L = 25 inches
 P_c = 100 psig
 ϕ_c = 2.54

Propellants:
 Hydrogen and Air
 Dynisco #9820

WAVE FORM OF UNSTABLE OSCILLATION

FIGURE 12